PERGAMON

Corrosion Science 45 (2003) 149–160

CORROSION SCIENCE

www.elsevier.com/locate/corsci

Anodising of Al 2024-T3 in a modified sulphuric acid/boric acid bath for aeronautical applications

L. Domingues [a], J.C.S. Fernandes [a], M. Da Cunha Belo [a], M.G.S. Ferreira [a,b,*], L. Guerra-Rosa [c]

[a] *Department of Chemical Engineering, Instituto Superior Técnico, 1049-001 Lisboa, Portugal*
[b] *Department of Ceramics and Glass Engineering, University of Aveiro, 3810-193 Aveiro, Portugal*
[c] *Department of Materials Engineering, Instituto Superior Técnico, 1049-001 Lisboa, Portugal*

Received 11 June 2001; accepted 29 March 2002

Abstract

A novel borate/boric/sulphuric acid anodising process is studied. The results show that the physical structure of the films is influenced not only by the bath used, but also and mainly by the substrate, i.e., Al 2024-T3 or Al. The corrosion resistance of the anodised specimens is satisfactory for practical applications and the fatigue resistance is not significantly different from that obtained with the traditional chromic acid anodising.

Keywords: Al 2024-T3 alloy; EIS; SEM; Anodising; Aeronautical industry

1. Introduction

Chromic acid anodising (CAA) is currently used in the aerospace industry in order to form oxide films on high strength aluminium alloys, such as Al 2024-T3. The use of traditional sulphuric acid baths is not recommended for these treatments, since they are detrimental for the fatigue life of the material.

* Corresponding author. Address: Department of Chemical Engineering, Instituto Superior Técnico, 1049-001 Lisboa, Portugal. Tel.: +351-21-841-72-34; fax: +351-21-840-45-89.
E-mail address: mgferreira@ist.utl.pt (M.G.S. Ferreira).

0010-938X/03/$ - see front matter
PII: S0010-938X(02)00082-3

CAA promotes the formation of a Al_2O_3 film incorporating some Cr(VI) and Cr(III) [1]. The film formed could be then sealed in hot water giving good corrosion resistance to the alloy or used unsealed as a base for painting or adhesive bonding.

Despite the good properties of the films obtained with this process, the use of Cr(VI)-containing treatments is unadvised from a health and environmental point of view, since it is toxic and carcinogenic.

Attempts have been made to replace the Cr(VI)-based treatments using oxianions with two oxidation states as the chromates, i.e., molybdates, vanadates and permanganates, although with limited success.

The present work uses an alternative for Al 2024-T3 anodising based on a sulphuric acid/boric acid/sodium borate (BSA) bath.

The structure of the films formed was examined using high resolution scanning field emission electron microscopy and compared with the one obtained for films formed on pure aluminium, which is generally envisaged as a thin non-porous barrier topped with a thick porous layer. The structure of the porous layer has been characterised as an array of columnar hexagonal cells each containing a central pore normal to the substrate surface [2].

Electrochemical impedance spectroscopy (EIS) was used to assess the film quality and corrosion resistance of anodised aluminium. Fatigue tests were carried out in order to evaluate the behaviour of the alloy anodised in BSA comparatively to the same alloy anodised in chromic acid and in the as-received condition.

2. Experimental

2.1. Anodising

Alloy 2024-T3 and commercial aluminium coupons with typical compositions shown in Tables 1 and 2, respectively, were used. The specimens were degreased with acetone, followed by etching in 3 $g\,l^{-1}$ NaOH solution (8 min) and desmutting in 50% (v/v) HNO_3 solution (30 s).

The anodising bath under investigation (BSA) consisted of a mixture of H_2SO_4 (15%) with a solution containing 0.5 M H_3BO_3 and 0.05 M $Na_2B_4O_7 \cdot 10H_2O$, in the proportion 70/30 (v/v).

Table 1
Typical composition (w/w%) of Al 2024-T3

Cu	Mg	Si	Fe	Cr	Zn	Mn	Al
3.80–4.90	1.20–1.80	0.00–0.50	0.00–0.10	0.00–0.10	0.00–0.25	0.30–0.90	Bal.

Table 2
Typical composition (w/w%) of Al (99.0%)

Cu	Si	Fe	Zn	Mn	Al
0.00–0.10	0.00–0.50	<0.70	0.00–0.10	0.00–0.10	Bal.

The current density used was 1.5 A dm^{-2} and the anodising time was 30 min. Two operating temperatures, 22 and 40 °C, were used. After anodising some coupons were left without further treatment, whereas others were sealed in deionised water at 100 °C for 30 min.

Specimens for fatigue tests were also prepared by anodising in a bath containing 50 g l^{-1} of CrO_3 ($T = 40$ °C, $i = 0.4$ A dm^{-2}) and then sealed in boiling water for 30 min.

2.2. Impedance measurements

The corrosion behaviour was studied in 3% NaCl solution by EIS. The equipment was a Solartron 1250 frequency response analyser connected to the cell via a Solartron 1286 electrochemical interface.

The measurements were carried out with three electrodes, at a d.c. potential slightly cathodic to the corrosion potential (E_{corr}—20 mV) to avoid deviations in the system linearity [3], by applying to the cell a 10 mV (rms) sine wave. The frequency range was 50 kHz to 5 mHz.

2.3. Fatigue measurements

Since the fatigue results are very time consuming they were carried out only on specimens anodised in the BSA bath at 40 °C, since a thinner coating should be preferable in terms of fatigue resistance.

For comparison, fatigue resistance was also determined on as-received and chromic acid anodised specimens. The alloy was submitted to tensile–tensile fatigue tests in air and at ambient temperature, in order to obtain S–N plots. Force sine waves with a stress ratio $R = F_{min}/F_{max} = 0.001$ were applied. The frequency changed between 10 and 25 Hz. The tests were carried out according to ASTM E 466-82 [4], using an INSTRON 8502 servohydraulic machine.

3. Results and discussion

Fig. 1 shows SEM photographs of transverse sections of non-sealed Al 2024-T3 specimens anodised in BSA at 22 and 40 °C. They allow the determination of the coating thickness, that is approximately 11 μm for the bath operated at 22 °C and 2.5 μm for the same bath at 40 °C. Higher magnification (160 000×) micrographs (Fig. 2) show in more detail the structure of these coatings. Linear continuous pores perpendicular to the specimen surface, as those reported in the literature for anodised aluminium [2], cannot be seen. The coatings have a non-orientated grain like structure with the grains separated by pores. In the case of the coating formed at higher temperature (Fig. 2b), the grains seem to have grown preferentially in one direction, revealing a lamellar shape. This type of structure seems to be a characteristic of the anodised films formed in this alloy independently of the electrolyte used for anodising [5].

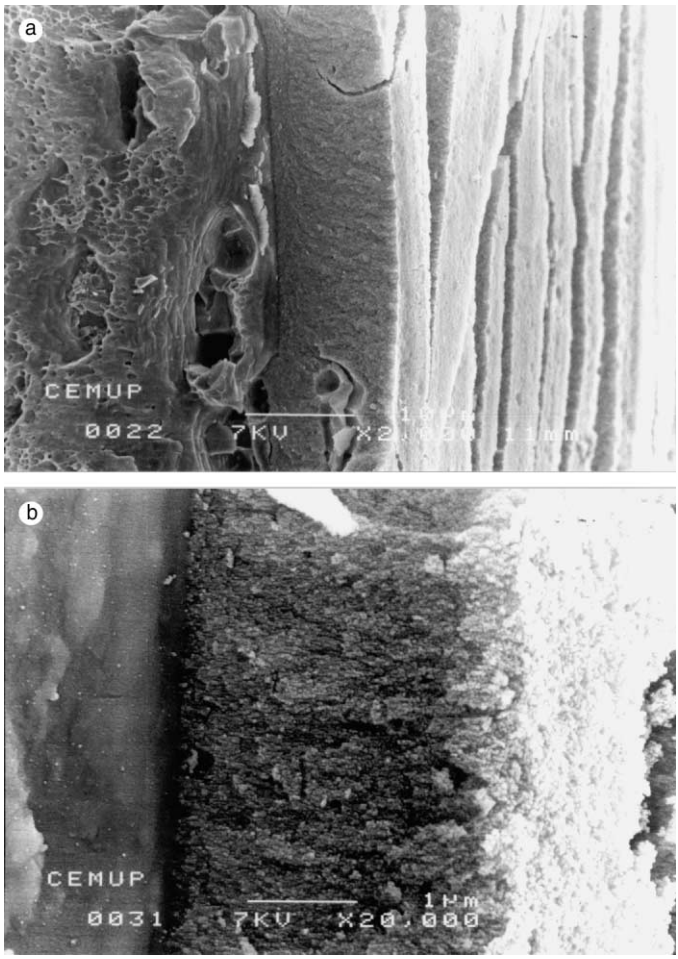

Fig. 1. Micrographs of transverse sections of anodised Al 2024 in BSA at temperatures of: (a) 22 °C (2000×), (b) 40 °C (20 000×).

The presence of a barrier layer in contact with the metallic surface could not be detected, which indicates that it should be very thin. However TEM observations reveal the presence of this layer [5].

The impedance results for 1 day and 7 days immersion in 3% NaCl solution of the specimens anodised with BSA at 22 and 40 °C are shown in Fig. 3. In every case the impedance values do not change significantly with time, which reveals a good corrosion performance of the specimens. In a similar manner there is no significant difference between the results obtained at 22 and 40 °C. This indicates that the EIS spectra in the measurement frequency range used, are mainly the result of the contribution of the barrier layer. Otherwise, as the thickness of the porous layer is

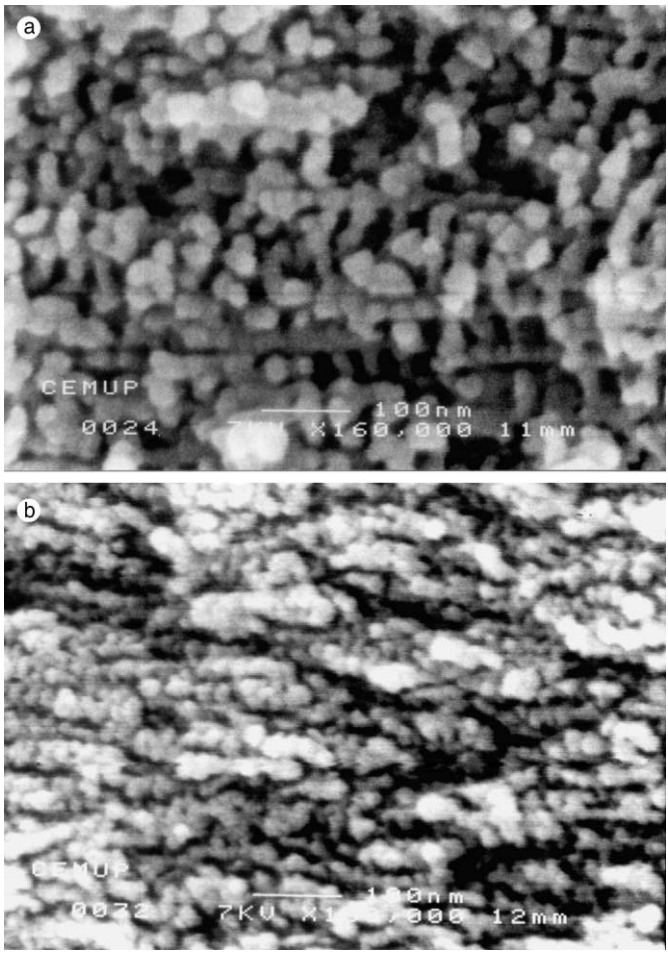

Fig. 2. Higher magnification (160 000×) of the micrographs in Fig. 1: (a) 22 °C, (b) 40 °C.

quite different, the impedance should also change. Thus, although the barrier layer is thin, it has an important role in the electrochemical response of the system.

Identical conclusion can be taken from impedance results obtained for specimens anodised for different times (e.g. 10 and 30 min), where the impedance spectra do not change with the porous layer thickness.

The analysis of the impedance spectra for short immersion times (Fig. 4), reveals that the porous layer is apparent at high frequencies, but when time elapses its impedance response vanishes. Thus a second time constant is visible for times less than one day, although after 3 h immersion its effect is already small. The explanation for this situation might be due to the fact that sealing only occurs superficially, in the external part of the porous layer, resulting in a short period of time the

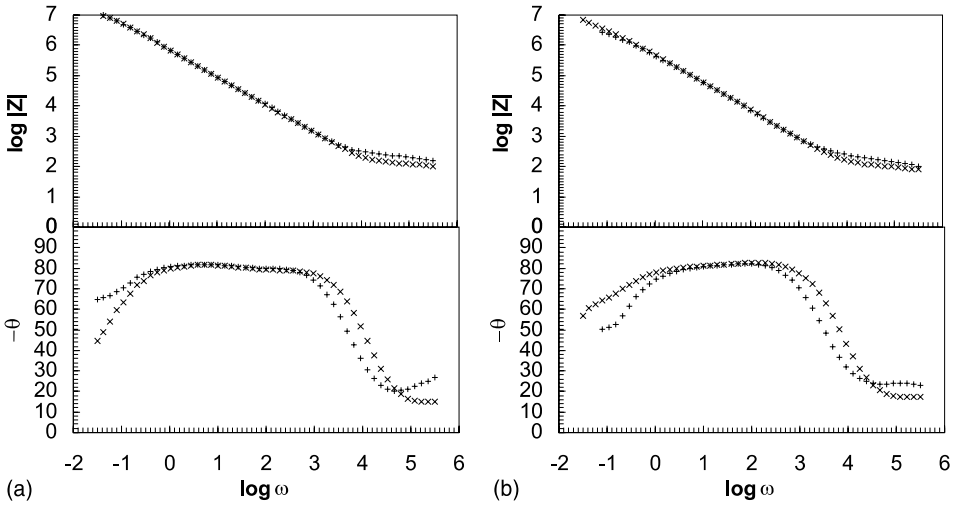

Fig. 3. Bode diagrams for specimens anodised in BSA solution at (a) 22 °C, (b) 40 °C (× = 1 day and + = 7 days of immersion in 3% NaCl solution).

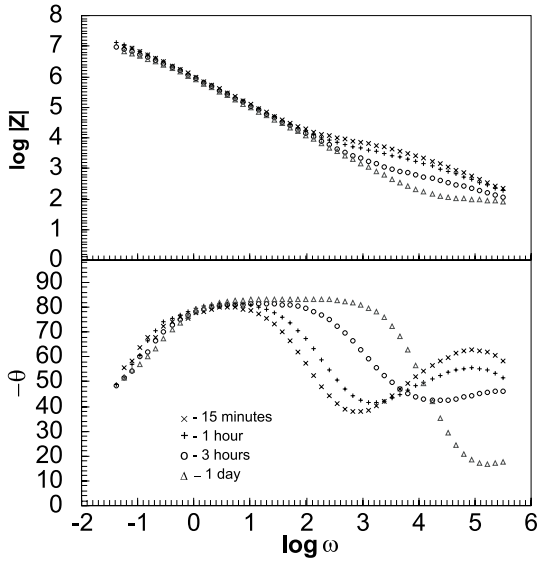

Fig. 4. Bode diagrams for Al 2024-T3 coupons anodised in BSA solution for 10 min and sealed (22 °C); different immersion times in 3% NaCl solution.

electrolyte is able to penetrate the sealed layers. After this, the response of the impedance measurements comes mainly from the barrier layer.

One time constant was also found by Mansfeld and Kendig [6] when sealing did not close the pores with hydrated oxides. The structure of the porous layer and the

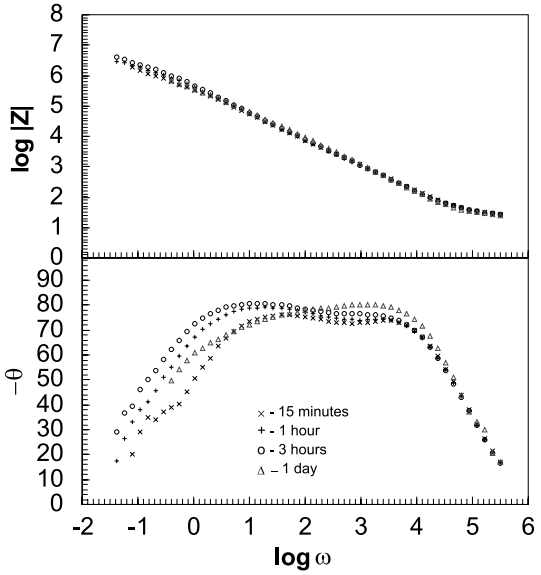

Fig. 5. Bode diagrams for Al 2024-T3 coupons anodised in BSA solution for 10 min and not sealed (22 °C); different immersion times in 3% NaCl solution.

quality of the water used in the sealing process seems to influence the nature of sealing. Thus waters containing lower concentration of SiO_2 and Cl^- could lead to a more compact hydration layer, originating two time constants for longer periods of time [5].

In the case of unsealed specimens the impedance results (Fig. 5) show that even for very short immersion times two time constants can hardly be distinguished. After 15 min immersion the electrolyte has already penetrated the unsealed layer, making the response of the porous film difficult to be observed.

Commercial pure aluminium (99%) anodised in the same solution (BSA), Fig. 6, reveals two time constants for the sealed specimens, even for long immersion times, which should mean a more effective sealing of the porous layer.

On the contrary the specimens with unsealed layers reveal clearly only one time constant, since the beginning of immersion. One plausible explanation is the pore structure, which in the case of pure aluminium is constituted by linear regular pores placed perpendicularly to the surface (Fig. 7), short-circuiting in a single way the barrier layer with the external electrolyte, whereas in the case of the alloy a tortuous pore morphology exists, making more difficult the access of electrolyte. It is the same pore morphology that is responsible for poorer sealing in the case of the Al 2024 alloy, since water penetration along the pores is difficult, slowing down the hydration of alumina in depth.

The above results agree completely with the physical models developed by Hitzig et al. [7] for inhomogeneous aluminium oxide layers. They showed that two time constants (Fig. 8), one related with the barrier layer and another one related with the

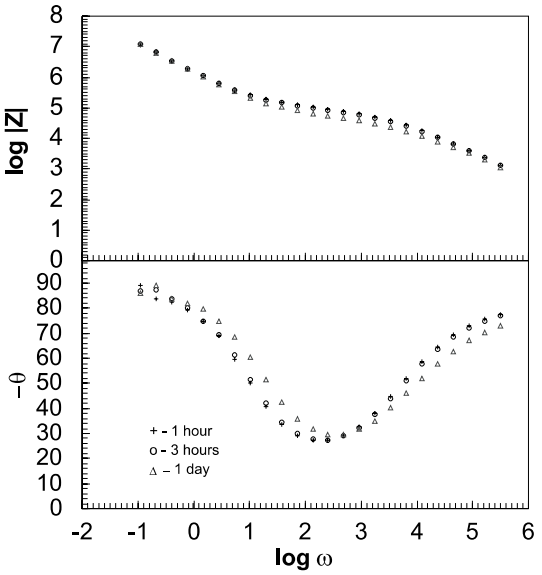

Fig. 6. Bode diagrams for commercial aluminium (99%) coupons anodised in BSA solution for 30 min and sealed; different immersion times in 3% NaCl solution.

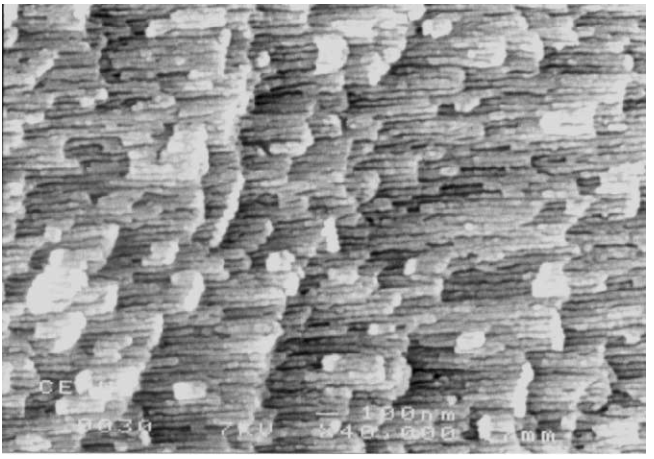

Fig. 7. Micrograph of transverse sections of anodised Al 99% in BSA at 22 °C (40 000×).

porous layer can only be clearly distinguished when a perfect oxide layer is present or the fraction of the surface covered with the oxide, θ, is very close to 1. If surface inhomogeneities resulting from deficient sealing of the porous layer occur, the

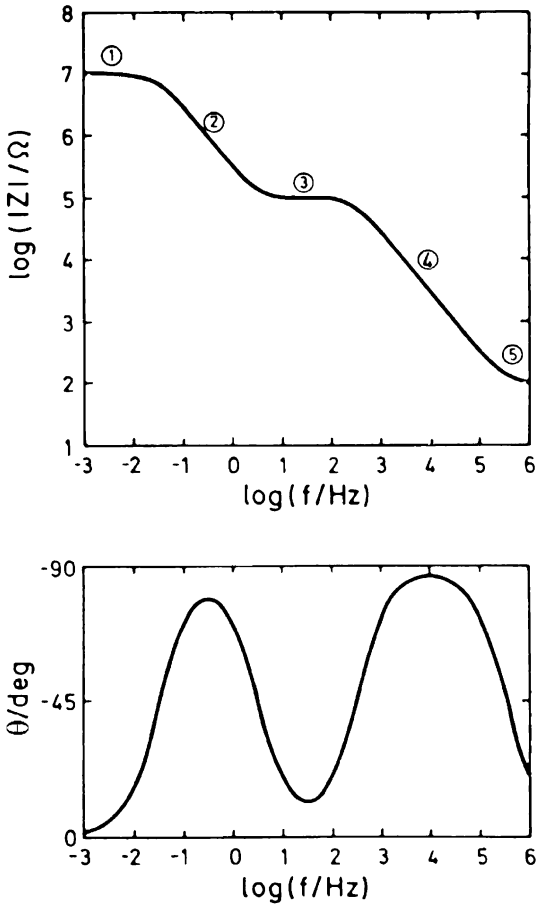

Fig. 8. Simulated Bode diagram for the equivalent circuit of anodised aluminium, showing the response of the porous and barrier layer [7].

plateau at intermediate frequencies in the $\log|Z|$ vs $\log\omega$ Bode diagram, the plateau related to the porous layer resistance, vanishes, appearing only the solution resistance (part 5 in Fig. 8) at high frequencies and the barrier layer resistance (part 1 in Fig. 8) at low frequencies. Moreover the capacitance line is shifted to lower values of $\log|Z|$ with values of capacitance exceeding the values of the porous layer and barrier layer capacitances (parts 4 and 2 of Fig. 8). When the barrier layer is attacked by localised corrosion, the value of the resistance measured at low frequencies should not be the barrier layer resistance, but instead the charge transfer resistance associated to the corrosion process. In the present case as for the period of time considered corrosion is not occurring and the value of the barrier layer resistance is

larger than 10^7 Ω, the resistance at low frequencies could not be measured. This is a limitation of the equipment used that does not allow measurements with accuracy higher than that value.

The degree of protection conferred by the oxide films formed under different experimental conditions has been assessed based on cabinet tests (i.e., salt spray tests) [8] and impedance measurements, at one single frequency or in a range of frequencies [7,9–13] in order to obtain the whole spectrum. In this latter case as very often a plateau is not observed at low frequencies for anodised samples even if they show pitting corrosion (since the charge transfer resistance is still very high and measurements at low frequencies become difficult), practical criteria have been established to assess the corrosion behaviour of these materials [6,14,15]. Most of them are based on the value of the impedance in the low frequency region. Thus, according to Mansfeld and Kendig [6], a damage function, D, which is defined as

$$D = \log\left(\frac{Z_0}{Z_t}\right)_{0.1\,\mathrm{Hz}} \tag{1}$$

is a useful measure of the corrosion susceptibility. Z_0 and Z_t are at 0.1 Hz the initial impedance value and the value of impedance for a certain immersion time, t, usually in 0.5 M NaCl solution. The value of t has been considered 7 days and a value of $D = 0$ represents perfect corrosion behaviour. In the present work a criterion previously used by the authors [15] is applied to predict whether or not the corrosion resistance of the anodised specimens is enough for practical applications. It is based on the value of the impedance data taken at $\omega = 10^{-1}$ rad s^{-1}, after 7 days of immersion in the testing solution. If this parameter is larger than 10^6 Ω cm^2, the coating is considered to have enough corrosion resistance for practical applications.

Applying this criterion to the results obtained for the new BSA bath, the value of $\log|Z|$ was monitored during 7 or more days. For both temperatures (22 and 40 °C) the above criterion was fulfilled, since that parameter was always higher than 6.5 (Fig. 9).

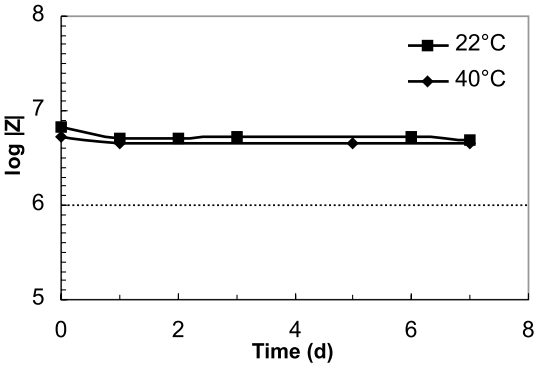

Fig. 9. Log $|Z|$ at $\omega = 10^{-1}$ rad s^{-1} vs time for specimens anodised in BSA at 22 and 40 °C (immersion in 3% NaCl solution).

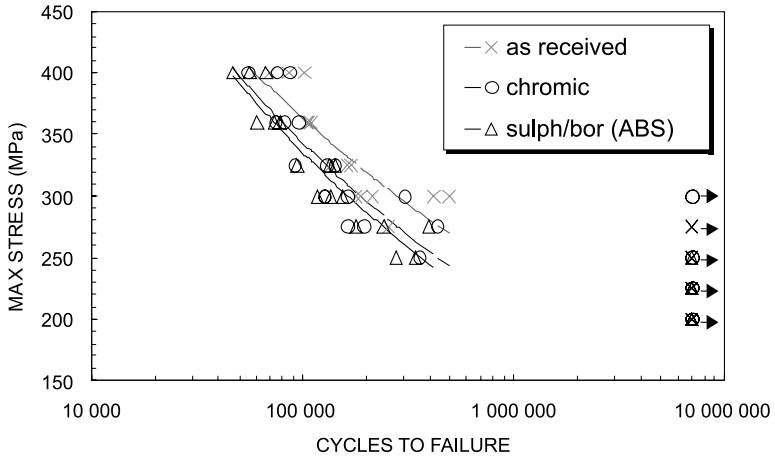

Fig. 10. S–N plots obtained for Al 2024-T3 in three different surface conditions: as-received, chromic acid anodised, ABS anodised.

Fig. 10 depicts the S–N plot obtained for specimens anodised with the BSA bath at 40 °C in tensile–tensile fatigue tests up to the fracture of the specimen. In the same figure and for comparison the same kind of plots obtained for the as-received alloy and standard CAA are also displayed. The results marked with arrows correspond to specimens that did not break up to 7×10^6 cycles.

The scattering of the results is typical of S–N plots for alloys of the type under study. From the analysis of the plots it is apparent that anodising induces a decrease of the fatigue resistance. The larger difference in behaviour is observed for stresses below 290 MPa. Comparing the BSA bath with the chromic acid bath it can be noticed that the specimens produced with the former are those that resist to lower maximum stresses. However, in any case the decrease in fatigue resistance is very low. This decrease can be characterised as $(S_{\text{ref}} - S)/S_{\text{ref}} \times 100$, where S_{ref} is the value of stress to fracture at 10^5 cycles for the reference treatment and S is the same value for the new surface condition. In particular, for BSA relatively to CAA, this ratio is $\sim$2%, which is much lower than the scattering range of the results.

4. Conclusions

Anodic oxide films produced in boric acid/sodium borate/sulphuric acid bath on Al 2024-T3 alloy depict a non-orientated grain like structure with the grains separated by pores. The pores are thus tortuous. This in opposition with films formed on Al 99% in the same bath where linear regular pores placed perpendicularly to the surface can be seen.

Sealing of the porous layer of these films in hot water seems to be more effective in aluminium than in the alloy.

Temperature at which anodising is carried out in BSA bath has a major impact on the coating thickness, although the structure is only slightly affected. The degree of protection conferred by the films is identical.

As revealed by EIS, the corrosion resistance of the anodised alloy obtained with the BSA bath at lower and higher temperature is identical and fulfils the practical criterion established for acceptance. However the film produced at 40 °C, as it is thinner, it is expected to originate materials with higher fatigue resistance.

The fatigue resistance of the BSA anodised specimens is slightly lower (~2%) than the chromic acid anodised ones, although this difference is within the experimental scattering of the results.

References

[1] A.J. Davenport, H.S. Isaacs, Corros. Sci. 31 (1990) 105.
[2] F. Keller, M.S. Hunter, D.L. Robinson, J. Electrochem. Soc. 100 (1953) 411.
[3] F. Mansfeld, J.C.S. Fernandes, Corros. Sci. 34 (1993) 2105.
[4] ASTM, Constant Amplitude Axial Fatigue Tests of Metallic Materials, American Society for Testing and Materials, E 466-82, Annual Book of ASTM Standards, 1984.
[5] L. Domingues, J.C.S. Fernandes, M.G.S. Ferreira, Internal Report, Instituto Superior Técnico, Lisboa, 2001.
[6] F. Mansfeld, M.W. Kendig, J. Electrochem. Soc. 135 (1988) 828.
[7] J. Hitzig, K. Juttner, W.J. Lorenz, W. Paastsch, J. Electrochem. Soc. 133 (1986) 887.
[8] Wong et al., United States Patent: 4 894 127, 1990.
[9] J.A. González, V. López, A. Bautista, E. Otero, X.R. Nóvoa, J. Appl. Electrochem. 29 (1999) 229.
[10] O.E. Barcia, J.L. Camara, O.R. Mattos, J. Appl. Electrochem. 17 (1987) 641.
[11] J. Hitzig, K. Jüttner, W.J. Lorenz, W. Paatsch, Corros. Sci. 24 (1984) 945.
[12] J.-P. Dasquet, D. Caillard, E. Conforto, J.-P. Bonino, R. Bes, Thin Solid Films 371 (2000) 183.
[13] F. Mansfeld, C. Chen, C.B. Breslin, D. Dull, J. Electrochem. Soc. 145 (1998) 2792.
[14] G. Buchheit, M. Cunningham, H. Jensen, M.W. Kendig, M.A. Martinez, Rapid Electrochemical Corrosion Testing of Chemically Passivated Aluminum Alloys, Corrosion 98, Paper no. 740, NACE, 1998.
[15] L. Domingues, J.C.S. Fernandes, M.G.S. Ferreira, I.T.E. Fonseca, Corros. Prot. Mater. 18 (2) (1999) 13.